EPJ Web of Conferences **67**, 02121 (2014)
DOI: 10.1051/epjconf/20146702121

Description of the three-phase contact line expansion

Tereza Váchová[1,a], Zuzana Brabcová[1] and Pavlína Basařová[1]

[1]Institute of Chemical Technology, Prague, Technická 5, 166 28 Prague, Czech Republic

Abstract. Knowledge of bubble-particle interaction is important in many industrial processes such as in flotation. While the collision (first interaction sub-process) between bubbles and particles is influenced only by hydrodynamic forces, the bubble behaviour during the attachment (second sub-process) is influenced both by hydrodynamic and surface forces. This work is focused on the study of the three-phase contact (TPC) line expansion during bubble adhesion on hydrophobic surface and on its experimental and mathematical description. The experiments were carried out in pure water where mobile bubble surface is expected. The rising bubble was studied in dynamic arrangement, whereas the stationary bubble was analysed in static arrangement. The attachment process was recorded using a high-speed digital camera and evaluated using image analysis. The diameter of the expanding TPC line as well as the dynamic contact angle was determined. Two approaches - the hydrodynamic and the molecular-kinetic - were used for mathematical description of the TPC line expansion. According to our results, the hydrodynamic model is suitable for the description of the initial fast phase of the expansion. The molecular-kinetic model was assessed as appropriate for almost whole range of TPC expansion. Parameters of the model were evaluated and compared for both types of arrangement.

1 Introduction

Bubbles and drops are entities of enormous practical interest since their interfaces are encountered in numerous industrial processes and applications of everyday life. Froth flotation is just one of the examples in which bubble-particle attachment plays a vital role. Due to its high separation efficiency, cost effectiveness and simplicity in operation and maintenance, flotation has been extended to other industries dealing with solid-solid and solid-liquid separations. Although flotation phenomena have been known for centuries, the pioneering systematic analysis on the fundamental steps of bubble-particle interactions in flotation could only be traced back to about 50 years ago. In contrast with the mentioned efforts stemmed from the needs of mineral flotation aimed at particles much smaller than bubbles, this project is focused on the investigation of behaviour of bubbles smaller in size with particles, which has not been satisfactorily covered yet. It seems that a good starting point for the small particle – large bubble interaction is the study of a bubble interaction with a flat wall, which represents a particle of infinite size. The bubble adhesion on the wall is controlled by the bubble ability to push out the liquid film, which separates them. For attachment, this film has to be thinned to the thickness of order of van der Waals and electrostatic forces range. These forces then destabilize the film, leading to its rupture and formation of the three-phase contact (TPC) line [1, 2]. Finally the three-phase contact line expands to the equilibrium. This project is focused on the study of the three-phase contact line during the bubble adhesion on the horizontal plane under two different experimental arrangements; stationary and dynamic. The experimental results are compared to model predictions, based on the hydrodynamic and molecular-kinetic theories.

Fundamentals of the hydrodynamic model were given by Cox [3], Huh and Scriven [4] and Voinov [5] whose described the TPC line from viewpoint of fluid dynamics. The hydrodynamic approach assumes only the viscous friction as a dissipative force; dissipation at the TPC line is neglected. The first models break down in a close proximity to the TPC line. Due to the application of "no-slip" condition of classical hydrodynamics the stress singularity occurs directly at the TPC line. To avoid such problem several models were proposed [4-6]. Generally, inner, intermediate and outer regions are distinguished for the description of the bubble close to the TPC line. The inner region applicable closest to the TPC line is determined by the slip length L_s of order of molecular distance. At distance greater than L_s the slip of the liquid along the solid surface occurs and stress singularity is removed. The TPC line motion in the inner region is influenced by molecular interactions and its shape could be represented by the microscopic contact angle θ_m. The

[a] Corresponding author: tereza.vachova@vscht.cz

size of the outer region is similar to bubble radius and is usually denoted as R. The outer region is also described by the macroscopic contact angle θ which is equal to the Young contact angle θ_{eq} [6, 7]. The intermediate region where viscous forces and surface tension operate is characterized by the dynamic contact angle θ_{dyn}. Such angle is dependent on the TPC line velocity and could be measured by available techniques [8]. After the equilibrium is established, the dynamic contact angle is equal to the Young contact angle. The stress influence is neither in the inner nor in the outer region so significant and contact angles θ_{eq} and θ_m remain during the TPC line motion almost constant. Phan [9] determined that the θ_m is almost equal to θ_{eq} for the glass/air bubble/pure water interface and this assumption is often used in the hydrodynamic model. Hocking, Rivers [7] and Cox [6] suggested the relation describing the difference between dynamic and microscopic contact angles.

$$q(\theta_{dyn}) - q(\theta_m) = \frac{\eta U}{\gamma} \ln\left(\frac{R}{L_s}\right) \quad (1)$$

Here η represents the liquid viscosity, U is the TPC line velocity and γ is liquid surface tension. The expression $q(\theta)$ for $\theta_{dyn} < 3\pi/4$ could be simplified as $\theta^3/9$ [5]. Then one could obtain:

$$\theta_{dyn}^3 - \theta_m^3 = 9\frac{\eta U}{\gamma} \ln\left(\frac{R}{L_s}\right). \quad (2)$$

When the microscopic contact angle is replaced by equilibrium contact angle [9], the combination of eq. (1) and (2) gives the following equation for the TPC line velocity and consequently for the radius of the TPC line r_{TPC} :

$$r_{TPC}(\tau) = \frac{\gamma}{9\eta \ln(R/L_s)} \int_0^t \left[\theta_{dyn}^3(\tau) - \theta_{eq}^3\right] \mathrm{d}\tau . \quad (3)$$

The term $\ln(R/L_s)$ appears here as an adjustable parameter. According to recent findings [9-11] the hydrodynamic model provides unreasonably large and thus physical unacceptable values of $\ln(R/L_s)$. It was concluded that the surface properties have to be considered to calculation of the TPC line velocity.

The molecular-kinetic model follows up the principles of surface chemistry [3, 12]. The first description of the model was published by Eyring [13] and by Yarnold and Mason [12]. The theory is based on the description of molecules and ions transport from one site of the solid surface to another one. Blake and Haynes [3] assume an existence of a large number of identical adsorption sites at which molecules or ions of gas can adsorb. The adsorption sites determine the equilibrium position, activation energy and due to the "hills and valleys" also the energy barrier which has to be overcome. The molecules and ions displacement takes place in both directions (forward, which is denotes as "+", and backward, denotes as "-") by jumping from one site to another [3, 14, 15]. According to the Eyring´s [12, 13] statistical treatment of the transport process the rate of displacements $K_\pm$ for both direction is given as

$$K_\pm = \left(\frac{k_B T}{h}\right) \exp\left(\frac{-\varepsilon_\pm}{k_B T}\right), \quad (4)$$

where $\varepsilon_\pm$ is the activation energy, k_B Boltzmann constant, h Planck constant and T denotes the temperature. The work W done to the system to overcome the energy barrier could be expressed by equation:

$$W = \gamma(\cos\theta_{dyn} - \cos\theta_{eq}). \quad (5)$$

Here the work W represents the unbalanced capillary force in the case when the dynamic and equilibrium contact angle differs from each other. The TPC line velocity is expressed as

$$U = \lambda(K_+ - K_-) \quad (6)$$

and according to [3] the radius of the TPC line is

$$r_{TPC}(\tau) = 2K\lambda \int_0^t \sinh\left[\frac{\gamma\lambda^2}{2k_B T}(\cos\theta_{dyn}(\tau) - \cos\theta_{eq})\right] \mathrm{d}\tau . \quad (7)$$

Here K is the frequency of molecular displacement with a typical value $10^6 - 10^7$ s^{-1} [3, 9, 10, 16]. Parameter λ is the average jumping distance and its value should be of order of molecular dimensions ($\approx$ 1 nm). It was found out that the molecular-kinetic model describes the TPC line motion very well. Agreement between calculated and experimental data is high and moreover, values of the adjustable parameters agree with the physical assumption [9, 11, 17].

Recently new models combining both approaches have been published [16, 18-20]. The basic assumption follows the idea that both the dynamic contact angle θ_{dyn} and the microscopic contact angle θ_m depend on the velocity. For the microscopic contact angle θ_m one could obtain [18]:

$$\theta_m(U) = \arccos\left[\cos\theta_{eq} - \left(\frac{2k_B T}{\gamma\lambda^2}\right) \mathrm{arcsinh}\left(\frac{U}{2K\lambda}\right)\right]. \quad (8)$$

After implementation of equation (8) into equation (1) and for $\theta_{dyn} < 3\pi/4$ one will get following equation [16]:

$$\theta_{dyn}^3 - \left\{\arccos\left[\cos\theta_{eq} - \left(\frac{2k_B T}{\gamma\lambda^2}\right) \mathrm{arcsinh}\left(\frac{U}{2K\lambda}\right)\right]\right\}^3 - \frac{9\eta U}{\gamma} \ln\left(\frac{R}{L_s}\right) = 0 . \quad (9)$$

The velocity U and thus also the TPC line radius are related both to microscopic (K, λ, L_s) and macroscopic (θ, R, η, γ) properties of the system. Although the molecular-kinetic model fits the experimental data very well, this approach gives more precise prediction of the TPC line velocity in its whole range [18].

2 Experiments

The experimental measurements were done in a special glass flotation cell (5.5 cm height, 8 cm width and 14 cm depth). The scheme of the experimental apparatus is given in figure 1. Single bubbles with diameters from 0.4 to 0.7 mm were created using a bubble generator built according to Vejražka [21]. The bubble collided with a microscope slide glass placed on a prism with a horizontal plane. The glass was silanized by dimethyldichlorsilan $(CH_3)_2SiCl_2$ provided by Sigma-Aldrich as the Silanization solution I. According to Zisman's method the solid surface energy γ_{sg} of silanised glass was 23.1 mN/m. Experiments were provided in pure distilled, de-ionised and de-mineralised water at 26 °C. The surface tension was 71.6 mN/m, pH value was 6.13 and conductivity 1.6 μS/cm. Equilibrium contact angle 97.8° for a sessile drop of pure water on this surface was measured using the ADSA technique.

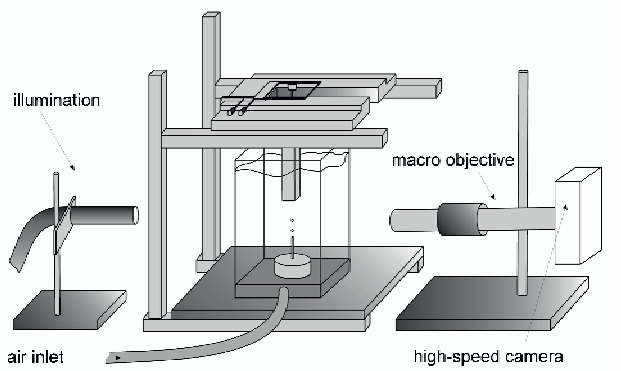

Figure 1. Scheme of experimental setup.

Whole experiment took place under two arrangements. Dynamic arrangement is characterized by bubble rising throught stagnant liquid before its collision with solid particle. In stationary arrangement the stagnant bubble collides with a solid surface. Whereas in dynamic arrangement the kinetic energy of the bubble plays an important role, in static arrangement the bubble kinetic energy is negligible. The collision process and the bubble adhesion were recorded using the high-speed digital camera Redlake Motion Scope M2 (2000 fps, resolution 1280 x 256 pixels, image calibration 2.44 - 4.94 μm/px). Around 1000 frames were taken for each sequence. The experimental terminal velocity of bubble rise was measured and compared with the prediction of Mei [22, 23] which is valid for pure water. The velocity calculated using this model is in close agreement with the experimental data, suggesting that the bubble interface is not contaminated with any additives or impurities.

Altogether, 6 sets of experimental data were obtained. These sets differ in bubble size (d_b = about 0.4, 0.6 and 0.7 mm) and experimental arrangement (dynamic x stationary). For one experimental set, adhesion process of ten bubbles was captured. Within one set of data, the variation of bubble size was about 1% and the maximum deviation from the mean did not exceed 3%. All images were evaluated using the image analysis software NIS-Elements when the bubble radius r_b and the TPC line diameter d_{TPC} were determined. Contact angles were measured using the modified ADSA methodology [24].

3 Results

The typical experiment is illustrated in figure 2. The adhesion of a bubble with diameter 0.57 mm (dynamic arrangement) and 0.60 mm (stationary arrangement) is given here. The time when the rupture of thin liquid film occurs was set as a zero time. After this moment the TPC line expansion was observed. After 0.1 s the equilibrium was almost achieved. The capturing was interrupted after 0.3 s. At this time the bubble shape was stable and the diameter of the TPC line together with contact angles did not change for more then 0.1 s.

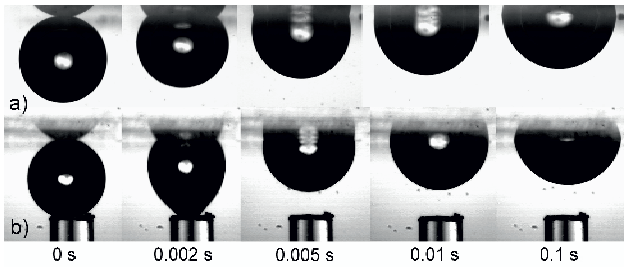

Figure 2. Sequence of photos showing the bubble adhesion on horizontal plane under dynamic (a) and stationary (b) experimental arrangement.

At first, the suitability of the hydrodynamic and the molecular-kinetic model was tested. The experimental radius of the TPC line r_{TPC} together with contact angle on both sides of the bubble was measured. Due to the fact that the difference between these two contact angles does not exceed 2°, their average value was taken as the dynamic contact angle θ_{dyn}. The equilibrium contact angle θ_{eq} was evaluated too. The average value was 94°. Finally, the parameter $\ln(R/L_s)$ of the hydrodynamic model (eq. 3) and parameters λ and K of the molecular-kinetic model (eq. 7) were evaluated using the regression analysis. The results for bubble with $d_b = 0.44$ mm are illustrated in figure 3, where the time dependence of radius of the TPC line r_{TPC} is given. The experimental data are depicted as circles; r_{TPC} calculated using the hydrodynamic model is illustrated as the dash line and r_{TPC} calculated using the molecular-kinetic model is illustrated as the full line. The hydrodynamic model describes the motion of the liquid near the interface and it could be appropriate for description of the first fast phase of the expansion. However, its parameter $\ln(R/L_s)$ is disproportionately high. If we consider the bubble radius r_b smaller then 0.5 mm and the slip length L_s close to 1 nm, the parameter $\ln(R/L_s)$ should reach the value close to 13. The value calculated from experimental data is about 100. Our observations are in accordance with previously published results [9-11] pointing out this drawback of the hydrodynamic model. On the other hand, the molecular-kinetic model fits experimental data very well. Both adjustable parameters λ and K reached values which are in a good agreement with theoretical

predictions [3, 9, 10, 16]. Therefore only the molecular-kinetic model was considered for next calculations.

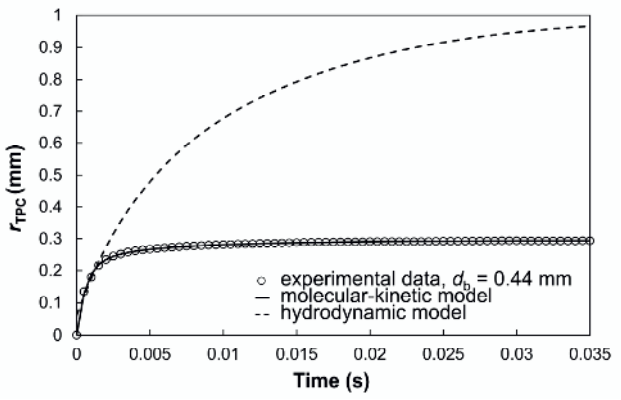

Figure 3. Expansion of radius of the three-phase contact line during the bubble adhesion. Experimental data (d_b = 0.44 mm) and comparison of molecular-kinetic and hydrodynamic model.

The calculated parameters λ and K of the molecular-kinetic model are summarized in table 1 together with sample variance and θ_{eq} for each bubble size and equilibrium angle.

Table 1. Molecular-kinetic model parameters values.

d_b (mm)	K (s^{-1})	λ (nm)	R^2	θ_{eq} (°)
Dynamic arrangement				
0.44	1.5 x 10^6	0.77	0.99	94
0.56	2.2 x 10^6	0.76	0.99	94
0.64	2.6 x 10^6	0.74	0.99	94
Stationary arrangement				
0.50	3.0 x 10^6	0.70	0.99	99
0.60	4.7 x 10^6	0.67	0.99	98
0.70	7.5 x 10^6	0.65	0.97	97

The comparison of experimental and calculated r_{TPC} is illustrated in figure 4 for both experimental arrangements. Very good agreement between experimental and calculated TPC line radius r_{TPC} is observed for both dynamic and stationary arrangement and moreover for all bubble diameters. Sample variances range from 0.97 to 0.99. The fitted parameteres λ and K correspond with theoretical predictions. Average jumping distance λ ranges from 0.65 to 0.77 nm which is in agreement with assumption of the order of molecular dimension (≈ nm). The frequency of molecular displacement K moves within the order of 10^6 s^{-1} which is physically correct and similar to previously published data [19, 25]. The molecular-kinetic model was determined as an appropriate one for almost the whole range of TPC expansion and can be thus used for the description of the TPC line motion.

When results for dynamic and stationary arrangement are compared one could observe the significant difference. For the stationary bubble the frequency of molecular displacement K is more than twice higher than for the rising bubble. Contrarily the average jumping distance λ decreases. It could be concluded that the bubble motion preceding the bubble adhesion has an appreciable influence on the TPC line dynamics.

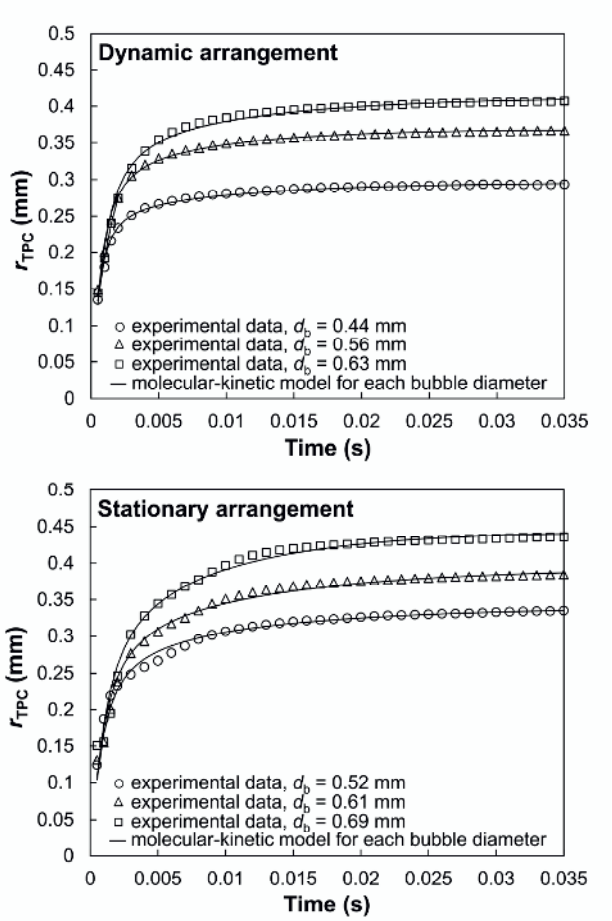

Figure 4. Comparison of experimental radii of the TPC line with molecular-kinetic prediction for dynamic and stationary experimental arrangement.

The parameters λ and K of the molecular-kinetic model are obtained by means of the regression analysis. The model should describe both the initial fast part and the following slow phase of bubble adhesion. Unfortunately the number of experimental points is significantly lower for the fast part of adhesion which is crutial for the TPC enlargement [26]. The influence of number of points (expressed as time dependence) on parameters λ and K is illustrated in figure 5 for both dynamic and stationary experimental arrangements. While parameter λ increases slightly with growing time interval, parameter K has decreasing trend. It declines considerabely, primarily in the first phase of the expansion. On the other hand, increase in points number results in substantial accuracy decrease in the crutial fast part. Therefore only the limited number of experimental points should be reccommended for the regression [26]. In this project the maximum time was 0.035 s. Parametres given in table 1 were calculated under this condition. Authors believe the accuracy to be sufficient.

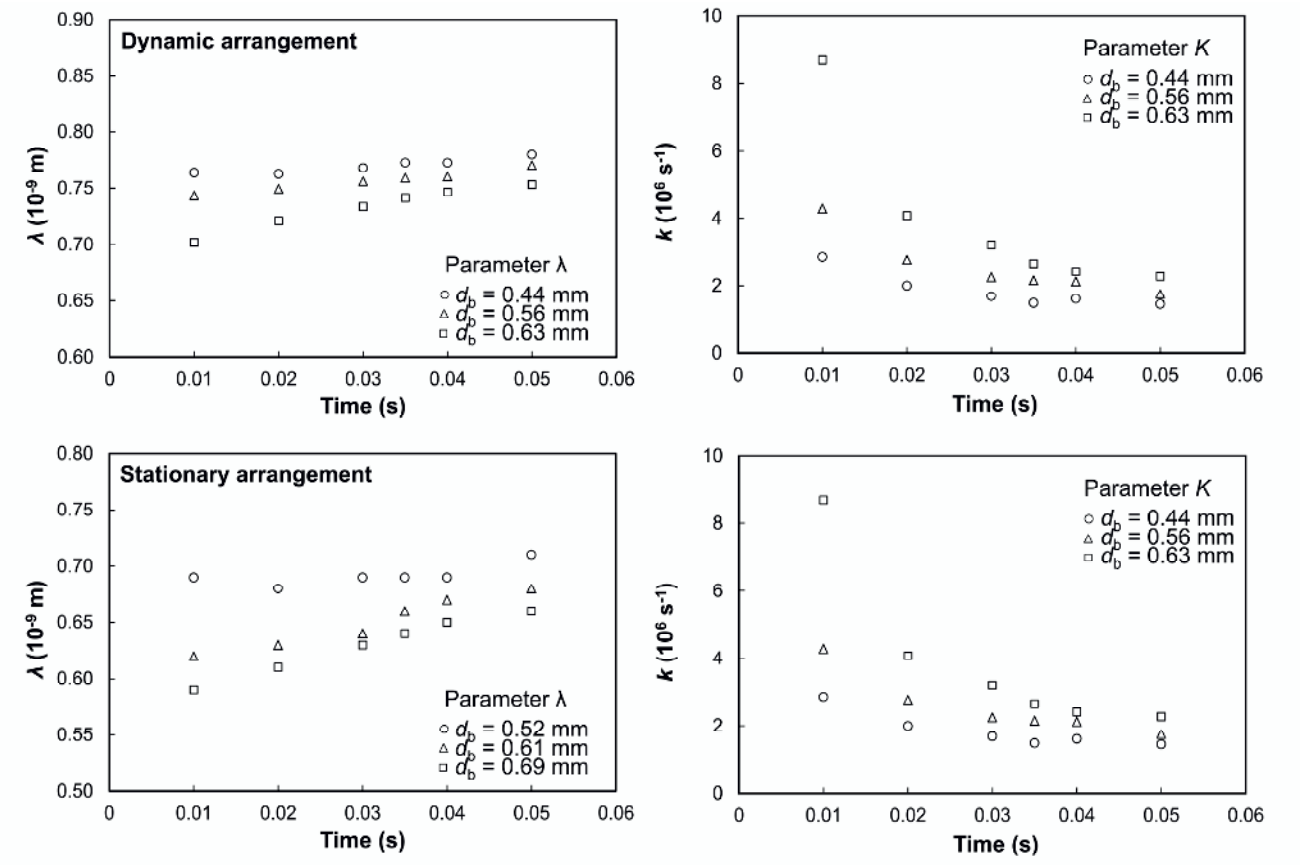

Figure 5. Time dependence of adjustable parameters λ and K of the molecular-kinetic model for dynamic and stationary experimental arrangement.

4 Conclusions

The expansion of the TPC line for a small bubble adhering on the horizontal hydrophobic surface was studied for the dynamic and the stationary experimental arrangements provided that the bubble surface is mobile. The experimental TPC radii and contact angles were obtained using image analysis. Mathematical models (hydrodynamic and molecular-kinetic) were tested for the theoretical description of the TPC line expansion. While the hydrodynamic model fails, the molecular-kinetic model describes experimental data with excellent agreement. Values of both parameters (the frequency of molecular displacement K and the average jumping distance λ) correspond to physical conditions. These parameters depend on bubble size and also vary for different experimental arrangements. Therefore it was concluded that the bubble motion preceding the bubble adhesion has an appreciable influence on the TPC line dynamics.

Acknowledgements

This work was supported by the Czech Science Foundation (project 101/11/0806) and by the Ministry of Education, Youth and Sports (project LD 13025) and by specific university research (MSMT no. 20/2013). Likewise the support from COST action MP1106 was appreciated.

References

1. A.V. Nguyen and H.J. Schulze, *Colloidal science of flotation*. first edn. (Marcel Dekker New York, 2004)
2. P.G. de Gennes, F. Brochard-Wyart, and D. Quéré, *Capillarity and wetting phenomena: drops, bubbles, pearls, waves*. first edn. (Springer New York, 2004)
3. T.D. Blake and J.M. Haynes, J Colloid Interf Sci. **30**, 421 (1969)
4. C. Huh and L.E. Scriven, J Colloid Interf Sci. **35**, 85 (1971)
5. O.V. Voinov, Fluid Dynamics **11**, 714 (1976)
6. R.G. Cox, J Fluid Mech. **168**, 169 (1986)
7. L.M. Hocking and A.D. Rivers, J Fluid Mech. **121**, 425 (1982)
8. D.Y. Kwok and A.W. Neumann, Adv Colloid Interfac. **81**, 167 (1999)
9. C.M. Phan, A.V. Nguyen, and G.M. Evans, Langmuir. **19**, 6796 (2003)
10. R. Fetzer and J. Ralston, J Phys Chem C. **113**, 8888 (2009)
11. A.V. Nguyen, et al., Miner Eng. **19**, 651 (2006)
12. G.D. Yarnold and B.J. Mason, Proc. Phys. Soc. B. **62**, 121 (1948)
13. S. Glasstone, K.J. Laidler, and H. Eyring, *The theory of rate processes; the kinetics of chemical reactions,*

viscosity, diffusion and electrochemical phenomena. first edn. (McGraw-Hill Book Company, inc. New York; London,, 1941)
14. B.W. Cherry and C.M. Holmes, J Colloid Interf Sci. **29**, 174 (1969)
15. F. Brochard-Wyart and P.G. de Gennes, Adv Colloid Interfac. **39**, 1 (1992)
16. S.R. Ranabothu, C. Karnezis, and L.L. Dai, J Colloid Interf Sci. **288**, 213 (2005)
17. T. Váchová, P. Basařová, and Z. Brabcová, Procedia Engineering. **42**, 1897 (2012)
18. P.G. Petrov and J.G. Petrov, Langmuir. **8**, 1762 (1992)
19. C.M. Phan, A.V. Nguyen, and G.M. Evans, J Colloid Interf Sci. **296**, 669 (2006)
20. J.G. Petrov and B.P. Radoev, Colloid Polym Sci. **259**, 753 (1981)
21. J. Vejrazka, et al., Fluid Dyn Res. **40**, 521 (2008)
22. R.W. Mei and R.J. Adrian, J Fluid Mech. **237**, 323 (1992)
23. R.W. Mei, J.F. Klausner, and C.J. Lawrence, Phys Fluids. **6**, 418 (1994)
24. Z. Brabcová, P. Basařová, and T. Váchová, Procedia Engineering. **42**, 358 (2012)
25. M. Schneemilch, et al., Langmuir. **14**, 7047 (1998)
26. T. Blake, Private comunication.